

**A&A manuscript no.**  
(will be inserted by hand later)

**Your thesaurus codes are:**  
**08.01.1 - 08.01.3 - 08.03.1 - 08.16.3 - ??**

**ASTRONOMY  
AND  
ASTROPHYSICS**  
11.11.2018

# Spectral evolution of and radiation energy generation by coeval stellar populations with different initial composition and chemical enrichment

Peeter Traat

Tartu Astrophysical Observatory, 61602 Tõravere, Estonia

Received date; accepted date

**Abstract.** Initial chemical composition of stars is, besides their mass, another key factor in stellar evolution. Through stellar lifetimes and impact on radiation output and nucleosynthesis of stars it is controlling both the pace of evolution of galactic matter/light and changes in their integrated observables and spectra. However, because of long-time scarcity of homogeneous stellar evolutionary data for compositions other than solar, or "normal", all the estimates of physical situation and global parameters for galaxy collective (radiation density, "global" star formation rate (SFR) etc.) have effectively remained being restricted to the assumption of normal composition and the composition-dependence of galactic properties ignored even when it should be obviously rather significant, e.g. in discussions of the main galaxy-formation epoch between  $z \sim 1 \div 10$ .

With our evolutionary synthesis codes we have performed extensive computations of temporal behaviour of photometric and spectral properties of stellar populations having different initial  $Z$  and varying IMF-s and SFR-s. Also, the production of most common nucleosynthesis elements He, C and O was followed. These computations have been performed on the basis of two available but different homogeneous multicomposition stellar evolution tracks grids by Geneva and Padova groups and the Kurucz model atmospheres (Kurucz 1993).

In given paper next to the discussion of overall effects of evolutionary differences we also present and comment the normalized per stellar mass unit standard tables of the detailed radiation energy output from stellar populations with different chemical composition, integrated over the whole lifetime of their stars, likewise the tables on He, C and O production. The energy production at different wavelengths per production of unit amount of  $^{16}\text{O}$  and heavy elements are tabulated in the function of the "metallicity"  $Z$ , the slope parameter  $n = x+1$  (sic!) of the initial mass function (IMF) and the lowest stellar initial mass boundary,  $M_{\text{cut}}$ , for stars evolving finally into black holes.

**Key words:** galaxies: evolution - stellar populations - chemical enrichment - spectral distributions

## 1. Introduction

Apart from the initial nucleosynthesis in the first  $\sim 10^3$  seconds after the Big Bang, what settled the primordial abundances of light elements (cf. Wagoner et al. 1967; Walker et al. 1991; Smith et al. 1993), the only source of the chemical enrichment of the matter in the post-recombination Universe has been the nucleosynthesis by stars, with its products mixed into the ambient medium by stellar ejecta during rapid mass loss stages and through stellar winds. This way stellar nucleosynthesis has been the major driving force behind all the subsequent evolution of stellar systems and the main generator of radiation energy and the cosmic background from the formation of very first stars up to the present epoch.

As known, rapid nucleosynthesis in hot matter following the Big Bang settles the initial He content,  $Y_0$ , and produces negligible amounts of  $^3\text{D}$ ,  $^6\text{Li}$ ,  $^7\text{Li}$ , Be etc. Cosmology cannot tell us about the exact time and redshift, when the first stars might have appeared in the Universe and therefore the first stellar systems started to form, but it is believed to have happened at redshifts around  $z \sim 10$  or even somewhat higher. Originally extremely deficient in heavy elements, the chemical composition of the matter of these primeval galaxies will evolve rather unsignificantly in low-mass low-density objects, but in the high-mass objects the enrichment proceeds rapidly. Consequently, the chemical composition differences should be of great importance, when the radiation of young galaxies is being analyzed or used to address the cosmological problems.

## 2. The era of first galaxies

Longstanding observational search for the primeval galaxies, going historically back to a paper by Partridge and Peebles (1967), has by now pushed the redshift limit for the directly observed starforming objects the farther and farther, with the most distant objects presently known having  $z \sim 7$ . Although seemingly quite rare objects at so high redshifts, the discovery of quasars at  $z > 6$  (presumably surrounded by stellar component and fainter galaxies) testifies, that galaxy formation process and birth of first stellar populations is in some cases going very intensively on even in that young the Universe, with age slightly less than 1 Gy. For the most distant quasar presently known, J1148+5251 with redshift of  $z = 6.419$  (Fan et al. 2003), Bertoldi et al (2003) give on the basis of measured dust emission for its parent protogalaxy an estimate of very impressive star formation, with the rate  $\sim 3000$   $M_{\odot}/\text{yr}$ . Many far-away galaxies have been discovered in quasar fields, some of them seem even to be rather evolved. For example, deep imaging with Keck telescope of the field around PC 1247+3406 (Soifer et al. 1994), having  $z = 4.897$ , and the  $z = 3.8$  radio galaxy 4C 41.17 (Graham et al. 1994) have revealed the hints of a population of red galaxies at magnitudes  $K \sim 21$  and fainter. Graham et al. point out that the closest companions to the 4C 41.17 are very red with their emission most likely caused by starlight, with lower limit to their age deduced from initial starburst 0.5 Gyr, and if sharing the same redshift with 4C 41.17, should have formed at  $z \gtrsim 8$ .

Another but indirect evidence of the ongoing star/galaxy formation at these and even higher redshifts is the absence of continuum absorption shortward of Ly  $\alpha$  in quasar spectra (Gunn-Peterson effect), what testifies that the intergalactic medium has been practically completely ionized starting from the very early epochs down to the present. This is generally attributed to the stellar/galactic processes be they supernova-driven winds either from luminous (Schwarz et al. 1975) or low-mass (Tegmark et al. 1993) high- $z$  young galaxies, cosmic rays (Ginzburg and Ozernoy 1965; Nath and Biermann 1993) or the photoionization by stellar (Songaila et al. 1990; Miralda-Escudé and Ostriker 1990) or quasar (Arons and McCray 1969) UV-radiation. Of course, in reality all these sources get combined in producing the observed outcome. More exotic explanations have also included cosmological blast waves (Ostriker and Ikeuchi 1983), decaying massive neutrinos (Sciama 1990) etc.

First discovered by Gunn and Peterson (1965), the constraints to the effect got further developed by a number of observers, e.g. by Giallongo et al. (1994). They deduced, measuring the average depression between Lyman absorption lines of the quasar BR 1202-0725 ( $z_{em} = 4.695$ ) the value of optical depth  $\tau \leq 0.02 \pm 0.03$  at  $z \simeq 4.3$  and, taking the quasars to be the prime ionizers of the gaseous medium and maximizing their known statis-

tics, the estimate for the density of the IGM  $\Omega_{IGM} \lesssim 0.01$ . Juxtaposition of that result with the mean baryonic density deduced either from HI Ly  $\alpha$  absorption at  $z = 1.9$ ,  $\Omega_b = 0.044$  (Tytler et al. 2004), or from D/H measurements in nearly pristine gas clouds on the basis of conventional Big Bang nucleosynthesis,  $\Omega_b = 0.0214 \pm 0.0020 h_{100}^{-2}$  (Kirkman et al. 2003, for the popularly accepted value  $H_0 = 71 \text{ kms}^{-1}\text{Mpc}^{-1}$  it gives  $\Omega_b = 0.0425 \pm 0.004$ ) indicates, that even at these very early times the dominant part of the baryonic matter had been confined into dense substructures, what occupied a rather limited fraction of the total volume. *Vice versa*, identifying these dense structures at least partly being young/primeval galaxies contributing to the ionizing UV-radiation at these and higher redshifts, it would be possible to satisfy the balance  $\Omega_{IGM} + \Omega_{gal} + \Omega_{HI} = \Omega_b$ , with  $\Omega_{gal}$  and  $\Omega_{HI}$  denoting the densities of galactic matter and neutral hydrogen clouds, respectively.

## 3. Spectrophotometric models

Integrated spectra are the main sources of information on the stellar content and interstellar medium of external galaxies farther than the Local Group. Being primarily built up by thermal radiation of stellar component, the integrated spectrum depends on its age, star formation rate, stellar mass spectrum and chemical composition distribution, but may also be heavily influenced by the reradiation and absorption by dust and heated gas in starbursts. Owing to specific frequency behaviour, the nonthermal component can be easily recognized, all the other factors work together in build-up of the spectrum in a complex manner.

Evolutionary modelling of galactic *spectra* was started by Bruzual (1983) more than two decades ago, but remained for most of that period mainly constrained to solar composition, due to both lack of homogeneous stellar evolutionary track sets for different metallicities, as also underlined in the abstract, as well as spectral libraries for nonsolar compositions. They became gradually available to the midst of 1990's. Presently there do exist two consistent track sets with sufficient range of metallicities - set for 6 compositions produced by Geneva group (cf. Meynet et al. 1994, and Charbonnel et al. 1996, with earlier references in these; a sixth, high-metallicity  $Z = 0.10$  composition got added to the set later by Mowlavi et al. 1998) and Padova tracks ( cf. Girardi et al. 1996, and references therein, Girardi et al. 2000 for stars of lower masses), the latter covering with 8 compositions practically all the observable and theoretically useful metallicity interval from  $Z = 0.0001$  until  $Z = 0.10$ . Both yet still pose some smaller problems for applications(ors) - Geneva tracks do not include for 4 non-solar compositions (except  $Z = 0.001$ ) past-RGB stages of evolution of low-mass stars  $M \leq 1.7 M_{\odot}$ , so these have to be added from other (and inhomogeneous) sources, it also has shorter range towards extremely metal-deficient abundances. Plus, the location

of stars with masses  $M < 0.8 M_{\odot}$  on and subsequent evolution from the zero-age main sequence is not available, it has to be taken elsewhere. Padova tracks are relatively free of so basic problematics, except of lack of stars  $M > 9 M_{\odot}$  in  $Z = 0.10$  subset, some minor irregularities arise also for  $Z = 0.001$  composition because they were computed with different radiative opacities.

The only set of model atmospheres, suitable for evolutionary spectral synthesis, has been produced by Kurucz (1993), covering spectral range 90 Å– 160  $\mu\text{m}$  for twenty compositions. It is known that since Kurucz models do not contain bands of some molecules, in the cool star region  $T_{\text{eff}} \leq 4500^{\circ}\text{K}$  improvements are needed, but being developed by a group associated with Uppsala, such more sound atmospheres for cool stars have not became available yet.

At the end of 1970-s and beginning of 1980-s, I developed a code package for computations of photometric evolution for stellar systems, using theoretical tracks and observational color indices and bolometric corrections for stars of different temperatures and luminosity classes. This package was somewhat complemented at the beginning of 1990-s as to allow on the basis of stellar atmospheres to compute spectral distributions for single populations as well as for the case of continuous star formation in model galaxies and to compute the photometry for filters within their passbands. With this package, I have performed a wide set of computations of photometrical and spectral population models with different chemistry and input physics (incl. also variations of stellar track sets). We have used both track sets in these studies of spectral evolution of stellar populations in function of their initial metallicity and star formation parameters. No gas emission/dust absorption has been considered in the models, since it is highly individual for galaxies.

Unfortunately, being made about ten years ago, the results of these computations have not been published in due fashion. On the basis of Padova tracks and isochrones a standardized grid of spectral data files has been released (Traat 1996) on a CD-ROM, produced as a collective effort to compile a database for galaxy evolution modeling. The short description of that grid has been published in the paper, accompanying that CD-ROM and describing its content (Leitherer *et al.* 1996).

That grid includes 1008 models and has the widest practically useful range of star formation prescriptions. It covers all the Padova set abundance range, i.e. eighth metallicities  $Z = 0.0001, 0.0004, 0.001, 0.004, 0.008, 0.02, 0.05$  and  $0.10$ . For each  $Z$  value that dataset includes

- six power law IMF-s of different slopes  $1.6 \div 3.5$ ,
- corresponding single-generation populations (instantaneous formation, "initial starbursts")
- populations with continuous/continuing star formation for those IMF-s with 4 SFR index values  $s = 0$  (constant SFR),  $s = 1$  (exponentially declining),  $s = 1.5$  and  $2$  (initially faster, later slower than the exponential SFR) and 5 star-formation timescales  $0.2, 1, 2, 5$  and  $15 \text{ Gy}$ .

Spectra were presented for 50 ages in the case of starburst populations and 20 ages for populations with continuous star formation. Ages range from  $0.003 \text{ Gy}$  to  $20 \text{ Gy}$ .

SFR has been parametrized by a power of the gas volume density (as introduced by Schmidt (1959)), with index  $s$  and time-scale  $t_0$ . In this context, the single-generation ("initial-burst") populations with their independency on the SFR/its power index form the limiting "starburst"  $t_0 = 0$  case.

#### 4. Discussion of the metallicity-dependent spectral data

In the context of model stellar populations and their comparison with observations, they fall broadly into two categories, the passive (initial starburst) and active star-forming populations, the first formed in simultaneous burst and lacking any subsequent star formation, the second characterized by ongoing star formation. Later evolution of passive populations is just pure stellar physics except the number distribution of stars by mass (IMF), so under assumption of perfectness of our knowledge of stellar evolution it depends solely on chemical composition and IMF parameters. Active populations, being a superposition of infinite number of passive ones, additionally need for their characterization the SFR with its parameters.

Spectral evolution of passive, initial-burst populations computed with six compositions available in the Padova stellar tracks grid is represented on Fig-s 1-2. The method used for their derivation consists of the integration of their output over stellar mass along the continuous isochrones, also, to ensure a perfect "coherence" in metallicity Kurucz model atmosphere flux tables were interpolated to the values of actual track set metallicities before assigning spectra to the stars.

General pattern of the behaviour of the passive populations is as follows. Were we having included a pre-main-sequence stage of stellar evolution with time-count set-in at the Hayashi border, with the result of massive stars reaching the main sequence shortly after formation and less massive ones only in  $0.1 \div 1 \text{ Gy}$ , we would have started the population with lower initial blue luminosities, with their maximal value reached the later the greater the IMF slope,  $n$ . As it is not the case here, the populations considered have a maximum luminosity at all wavelengths at the onset, its absolute value dropping with the lowering of the number of massive stars in the IMF ( $\equiv$  increase of  $n$ ) and the monotonous decline of luminosity with time. The influence of  $n$  on the spectrum is the most easily understandable factor, since its growth causes the mechanical decline of the massive end of the IMF and, respectively, the overall mechanical decrease of the spectrum level towards shorter wavelengths and rise towards infrared, with

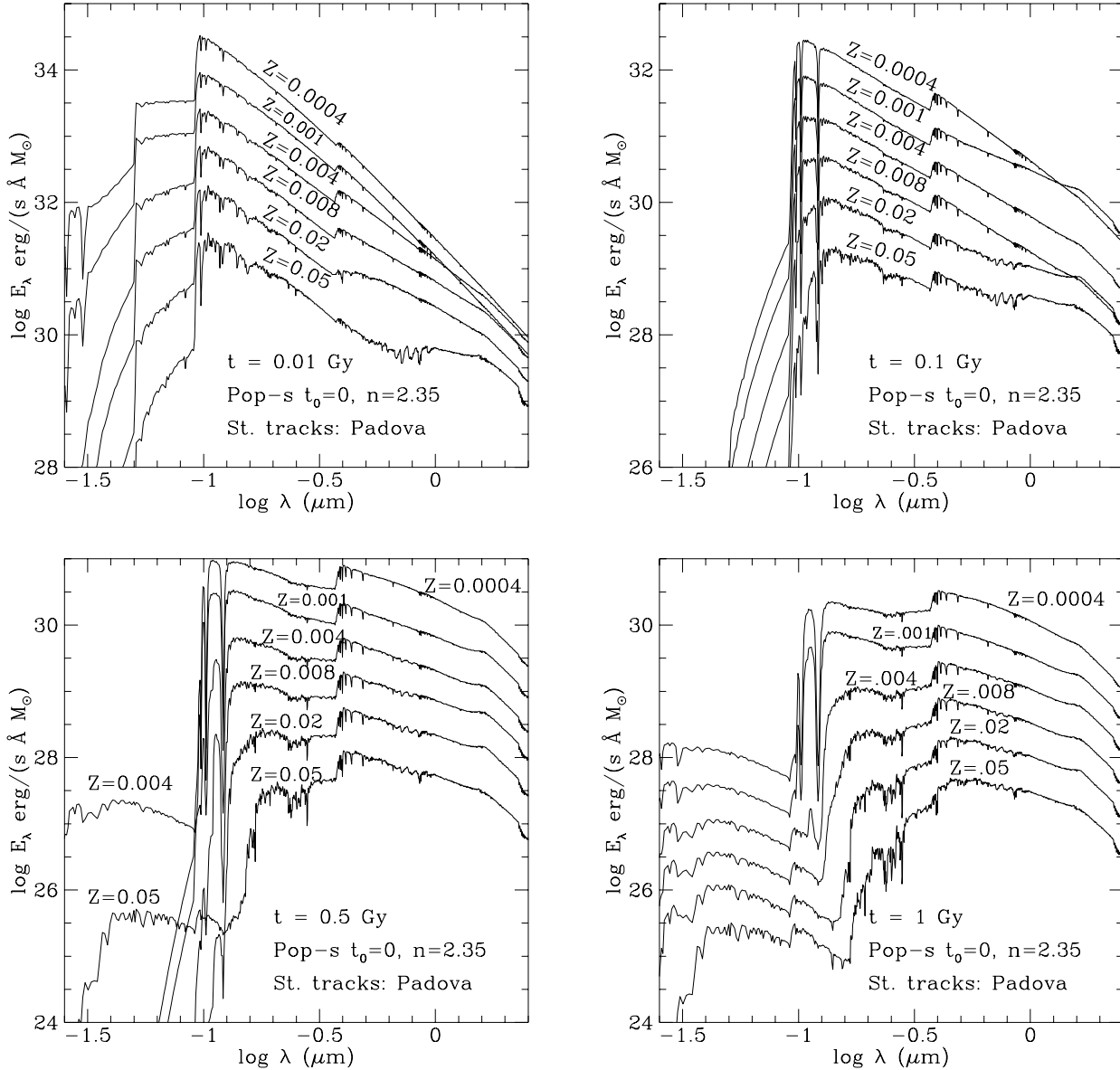


**Fig. 1.** Evolution of spectra of initial burst stellar populations with different metallicities. The  $Z = 0.0004$  spectrum has a correct location in  $\log E_\lambda$ , all the others have shifted downwards by additional 0.5 dex in respect of the previous one, with maximum shift  $-2.5$  in the  $Z = 0.05$  case.

the midst of the optical region being the approximate borderline (Fig. 3b). Both  $Z$  (Fig-s 1-2) and the age (Fig. 3a) work in the same direction, the short wavelength region becoming progressively eroded with their growth, and the more, the shorter the wavelength. However, with the rise of  $Z$  and the enhancement of absorption in metallic lines in UV the bulk of energy reradiated in the optical and near-infrared is increasing with the definite net result that the spectrum level at  $\lambda \geq 1 \mu\text{m}$  is for all ages progressively higher for higher metallicities. So a sufficiently long baseline for spectral or multicolor photometry coverage (plus some improvement of precision of both theory and obser-

vations) could probably resolve the age-metallicity degeneracy, I think a theoretical calibration might be attempted after the release of improved cool-star atmospheres.

There are yet some more noteworthy details pointed out on Fig-s 1-2 like the extremely rapid time evolution of the  $\text{He}^\circ$  continuum below 504Å and bit shallower change of the Lyman jump, making both of them theoretically good age estimators for the extremely young stellar populations. Fig. 3a is also embedding a reference to a specific peculiarity of the Padova track system: the high-metallicity population includes a hot AGB-*manque* ( $\equiv$ naked stellar core) stellar evolution phase, stars in this stage are the

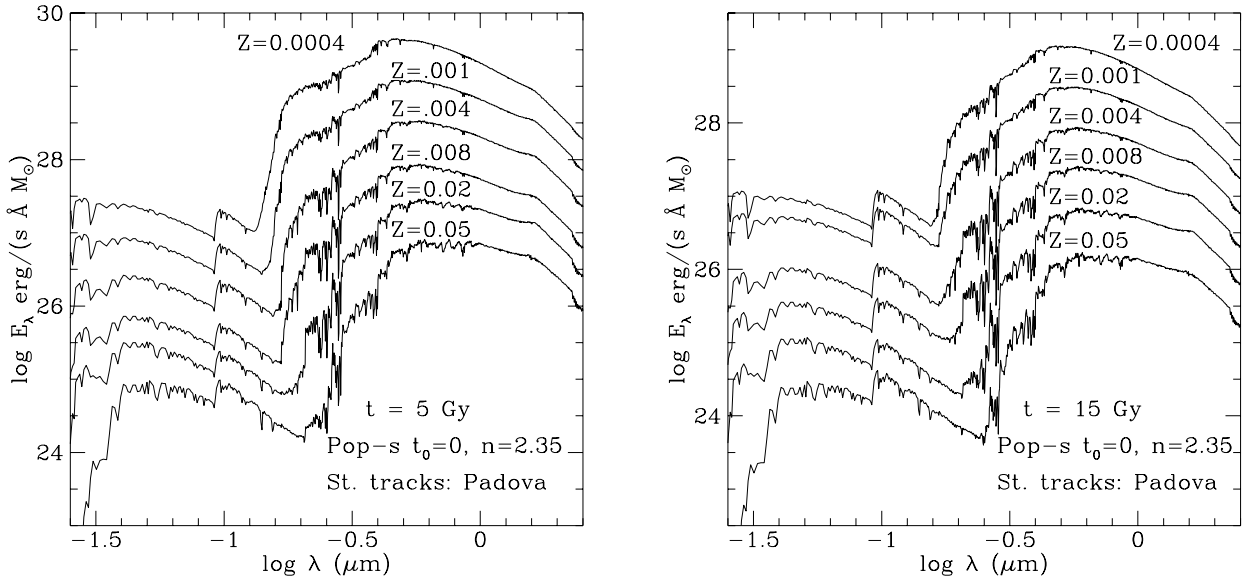


**Fig. 2.** (continuation of Fig. 1). Spectra of the same initial burst stellar populations at very old ages 5 and 15 Gy. Shifts on graphs are as indicated in caption to Fig. 1.

cause of the UV-flux upturn at ages  $\geq 10$  Gy. This interesting result is in full detail covered by the authors of tracks (Bressan et al. 1994).

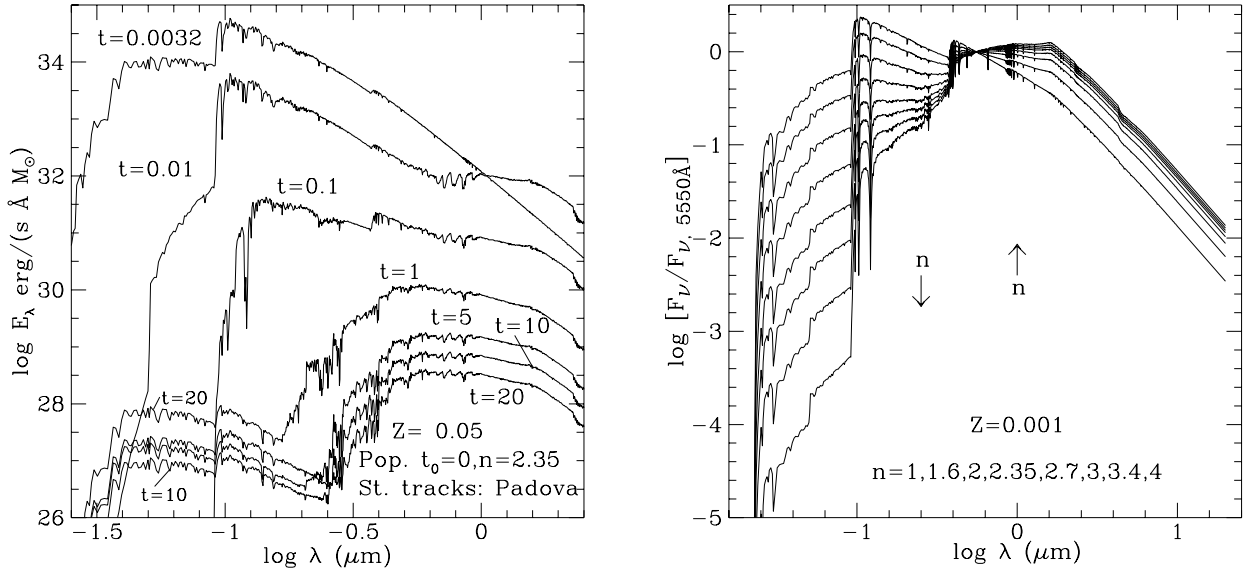
Spectral evolution of active populations is governed to a large extent by the SFR shape (i.e. power index  $s$  in the case here) and star-formation timescale,  $t_0$ . The reddest limiting case for both the spectrum and colors being the passive  $t_0=0$  population, the active population with the given  $s$  forms during its youth stars the slower the larger  $t_0$  value is, but has higher star-formation intensity and bluer colors at later epochs. The limits to what extent the selection of the functional form parameter  $s$  may influence the spectrum are approximately the same, the dependence of spectral evolution on  $s$  being for one parameter set illustrated on Fig. 4a ( $s=0 \equiv$ constant,  $s=1 \equiv$ exponentially declining star formation rate). The scale of impact depends also on the age of the population, in the  $s=0$ ,  $t_0=1$  Gy model the star formation has had an duration of first 1 Gy and not been working for 4 Gy-s until our time of observation, it makes the population spectra red and close to that of a passive population at the same age, 5 Gy. Right panel depicts the temporal evolution of an active stellar population with a quite extended timescale, so although both its colors and spectrum are slowly evolving to red, no impressive changes next to its overall absolute decrease are evident, even the UV-branch keeping nearly the same level in respect to the optical region, as a result of the continuing star formation at the levels not drastically differing from those in earlier stages.

## 5. Metallicity and radiation output in specific wavelength ranges

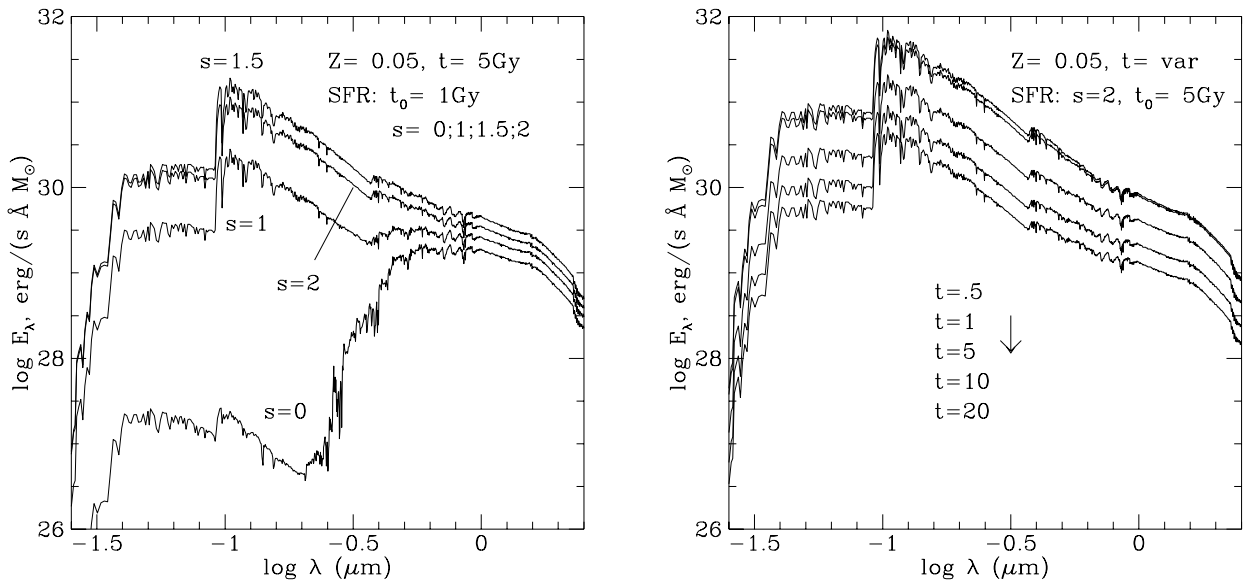
Metallicity growth affects the stellar evolution in two ways: first, making stars cooler and dimmer, secondly, redistributing their flux through opacity growth at short wavelengths towards longer wavelengths. So the summative result of  $Z$  rise on the composite spectrum of a stellar population is the progressive erosion of flux in ultraviolet region, and the faster, the shorter the wavelength. However, with the growth of  $Z$  and the enhancement of absorption in metallic lines in UV the bulk of energy reradiated in the optical and near-infrared is increasing with the definite net result that the spectrum level at  $\lambda \geq 1 \mu\text{m}$  is for all population ages progressively higher for higher metallicities.

Table 1 gives a general quantitative review of the extent of metallicity effects in different spectral regions for populations with different mass function slopes  $n$ . Time is eliminated by integration over the lifetimes of stars, population mass is scaled to the unit amount of mass in very massive stars  $M \geq 10 M_\odot$ , Geneva set of tracks (5 compositions, the  $Z = 0.10$  subset was not included) was used. These data testify, that composition-caused flux changes can be rather impressive, extending to factor of 10 in far-UV and  $\sim 2$  in infrared.

As to illustrate metallicity effects graphically, we also provide a couple of examples on Fig. 5, computed with Padova tracks. On the left panel of this figure we have plotted computed spectra of coevally formed stellar populations (so-called *initial burst* populations) with 8 different initial metallicities  $Z$ , having the same ages 1 Gy.



**Fig. 3.** *Left panel:* Age dependency of high-metallicity initial-burst population spectrum. *Right panel:* Impact of the IMF slope  $n$  on the total radiation energy output of a stellar population, integrated over its lifetime. Given panel is based on the Geneva tracks, distributions are normalized at 5550 Å. Arrows indicate the direction of growth of  $n$ , as to facilitate identification of curves.



**Fig. 4.** *Left panel:* Spectral evolution of a stellar population with continuing star-formation, having time-scale  $t_0 = 5$ . In the given  $s=2$  case half of the matter will during  $t_0$  be converted to stars. *Right panel:* Influence of the SFR time behaviour differences, as introduced by its power index  $s$  values, on the spectrum of a  $Z = 0.05$  population with continuous star formation.

**Table 1. Time-integrated energy fluxes** of coeval stellar populations with different IMF slopes and metallicities, per 1  $M_{\odot}$  in massive stars  $10 \div 120 M_{\odot}$ . Flux units  $10^{52}$  erg, flux fractions  $f_i$  computed for intervals 90.9-395 Å, 395-995 Å, 995-1995 Å, 1995-3590 Å, 3590-7490 Å, 0.749-4.99  $\mu\text{m}$  and 4.99-160  $\mu\text{m}$ .

n	Z	L	$f_1$	$f_2$	$f_3$	$f_4$	$f_5$	$f_6$	$f_7$
1.0	0.001	0.2944	.0792	.2585	.4691	.1090	.0635	.0206	.0002
	0.004	0.2977	.0503	.2429	.4932	.1153	.0695	.0284	.0002
	0.008	0.2896	.0383	.2465	.5128	.1170	.0590	.0262	.0003
	0.020	0.2629	.0243	.2408	.5265	.1172	.0539	.0368	.0005
	0.040	0.2305	.0096	.2012	.5476	.1367	.0659	.0385	.0005
1.6	0.001	0.3169	.0579	.2025	.4809	.1239	.0911	.0434	.0004
	0.004	0.3147	.0365	.1902	.4896	.1263	.0988	.0579	.0006
	0.008	0.3074	.0271	.1880	.5032	.1287	.0919	.0603	.0007
	0.020	0.2824	.0166	.1799	.5020	.1256	.0888	.0859	.0012
	0.040	0.2487	.0067	.1527	.5175	.1412	.0962	.0844	.0012
2.0	0.001	0.3897	.0376	.1405	.4561	.1388	.1393	.0868	.0009
	0.004	0.3746	.0239	.1339	.4546	.1365	.1444	.1055	.0012
	0.008	0.3678	.0174	.1296	.4578	.1375	.1420	.1144	.0014
	0.020	0.3458	.0103	.1201	.4352	.1291	.1419	.1611	.0023
	0.040	0.2997	.0043	.1052	.4519	.1415	.1441	.1509	.0021
2.2	0.001	0.4691	.0274	.1064	.4253	.1459	.1741	.1197	.0013
	0.004	0.4399	.0176	.1027	.4200	.1411	.1772	.1397	.0016
	0.008	0.4337	.0127	.0982	.4162	.1403	.1775	.1533	.0019
	0.020	0.4159	.0073	.0888	.3811	.1278	.1778	.2141	.0030
	0.040	0.3538	.0032	.0799	.4000	.1388	.1782	.1973	.0027
2.35	0.001	0.5620	.0205	.0823	.3947	.1502	.2029	.1477	.0016
	0.004	0.5159	.0133	.0805	.3872	.1436	.2049	.1684	.0019
	0.008	0.5106	.0095	.0762	.3779	.1411	.2070	.1861	.0023
	0.020	0.4985	.0053	.0674	.3346	.1249	.2063	.2578	.0037
	0.040	0.4166	.0024	.0621	.3547	.1350	.2066	.2359	.0032
2.5	0.001	0.6974	.0148	.0613	.3599	.1532	.2319	.1769	.0020
	0.004	0.6256	.0097	.0607	.3505	.1452	.2336	.1980	.0023
	0.008	0.6221	.0068	.0568	.3360	.1405	.2372	.2201	.0027
	0.020	0.6198	.0037	.0490	.2864	.1204	.2340	.3021	.0043
	0.040	0.5075	.0017	.0464	.3071	.1298	.2355	.2757	.0037
2.7	0.001	0.9767	.0090	.0391	.3115	.1551	.2681	.2148	.0024
	0.004	0.8492	.0060	.0394	.2997	.1458	.2706	.2358	.0027
	0.008	0.8506	.0041	.0363	.2793	.1377	.2754	.2640	.0032
	0.020	0.8719	.0022	.0303	.2255	.1126	.2666	.3577	.0050
	0.040	0.6937	.0010	.0297	.2451	.1211	.2717	.3270	.0044
3.0	0.001	1.7551	.0038	.0183	.2447	.1540	.3122	.2641	.0030
	0.004	1.4602	.0026	.0188	.2295	.1437	.3183	.2839	.0032
	0.008	1.4817	.0017	.0169	.2035	.1306	.3229	.3206	.0038
	0.020	1.5820	.0009	.0133	.1510	.0993	.3025	.4269	.0060
	0.040	1.2094	.0004	.0138	.1660	.1063	.3152	.3931	.0052
3.4	0.001	4.2012	.0011	.0060	.1768	.1485	.3510	.3130	.0036
	0.004	3.3257	.0007	.0063	.1585	.1382	.3636	.3290	.0037
	0.008	3.4400	.0005	.0054	.1303	.1191	.3651	.3752	.0044
	0.020	3.8395	.0002	.0040	.0867	.0828	.3286	.4907	.0069
	0.040	2.8204	.0001	.0044	.0948	.0875	.3505	.4567	.0060
4.0	0.001	16.8714	.0002	.0010	.1147	.1383	.3811	.3604	.0043
	0.004	12.6020	.0001	.0011	.0950	.1293	.4026	.3678	.0041
	0.008	13.4144	.0001	.0009	.0693	.1037	.3968	.4243	.0050
	0.020	15.6599	.0000	.0006	.0396	.0647	.3416	.5457	.0078
	0.040	11.1299	.0000	.0007	.0415	.0662	.3711	.5137	.0067

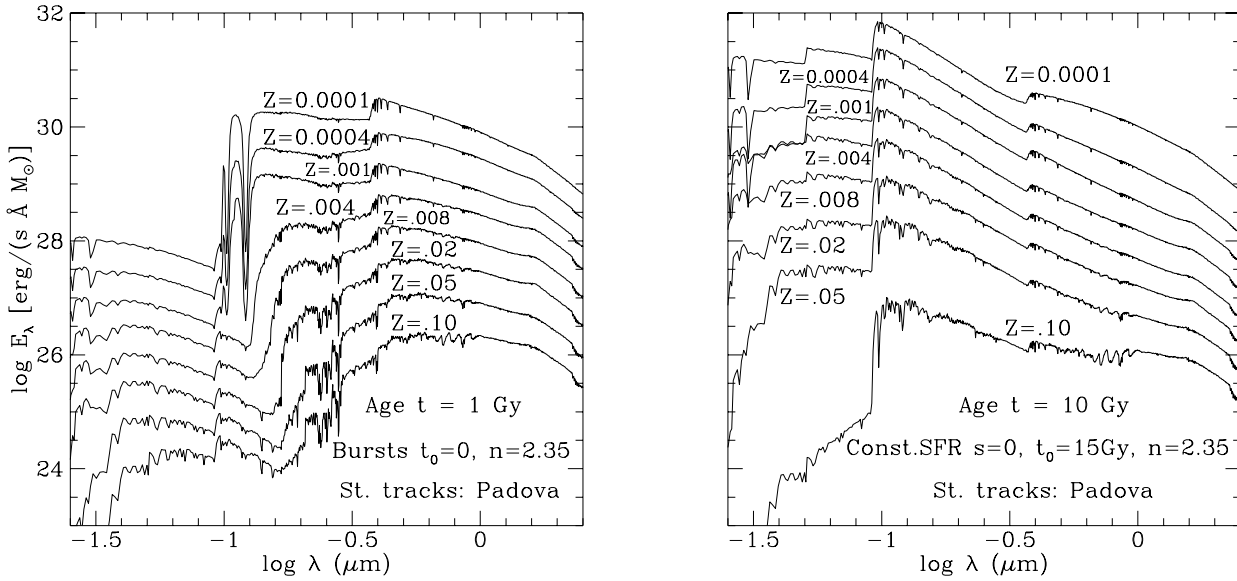


**Fig. 5.** Composition dependence of spectra of stellar populations: coevally formed young stellar populations (age 1 Gy, *left* panel) and old populations with constant SFR (age 10 Gy, *right* panel).

Such comparatively blue spectra are typical for medium-aged star clusters of assumed chemical compositions, or might be relevant to different parts inside young elliptical galaxies with ages somewhat exceeding 1 Gy. The flux of models is scaled to the unit mass in luminous stars with masses  $M > 0.6 M_{\odot}$ , the IMF in these graphs is a power-law with slope  $n = -2.35$  ("Salpeter" value). The most metal-deficient,  $Z = 0.0001$  spectrum has a correct location in  $\log E_{\lambda}$ , all the others have been successively shifted downwards by additional 0.5 dex, with maximum total shift  $-3.5$  for the  $Z = 0.10$  case. On the right panel the spectra of old, 10 Gy stellar populations, are plotted, in which star formation is continuous and proceeds with a constant, time-independent intensity over the eon  $t_0$ . Given case might be considered as a kind of approximation to late spirals or irregulars, since in many of these actual SFR-s do not seem to significantly differ from the mean average over their past. Notice, however, that due to the actively continuing star formation the ultraviolet flux of models keeps sizable. The growth of metal content sharply reduces the flux at shorter wavelengths, as also on the left-panel plot.

## 6. Nucleosynthesis

The tabulated nucleosynthesis of He, C and O will be available in replacement paper to this first draft!

## References

Arons J., McCray R., 1969, *Astrophys. Lett.* 5, 123

Bertoldi F., Cox P., Neri R., Carilli C.L., Walter F., Omont A., Beelen A., Henkel C., Fan X., Strauss M.A., Menten K.M. 2003, *A&A* 409, L47

Bressan, A., Chiosi, C., Fagotto, F. 1994, *ApJS*, 94, 63

Bruzual, G. 1983, *ApJ*, 273, 105

Charbonnel C., Meynet G., Maeder A., Schaller G., Schaerer D., 1993, *A&AS* 101, 415

Charbonnel C., Meynet G., Maeder A., Schaerer D., 1996, *A&AS* 115, 339

Fan X., Strauss M.A., Schneider D.P., Becker R.H., White R.L., Haiman Z., Gregg M., Pentericci L., Grebel E.K., Narayanan V.K., Loh Y., Richards G.T., Gunn J.E., Lupton R.H.; Knapp G.R., Ivezic Z., Brandt W.N., Collinge M., Hao L., Harbeck D., Prada F., Schaye J., Strateva I., Zakkamska N., Anderson S., Brinkmann J., Bahcall N.A., Lamb D.Q., Okamura S., Szalay A., York D.G. 2003, *Astron.J.*, 125, 1649

Fagotto F., Bressan A., Bertelli G., Chiosi C., 1994, *A&AS* 105, 39

Giallongo E., D'Odorico S., Fontana A., McMahon R.G., Savaglio S., Cristiani S., Molaro P., Trevese D., 1994, *ApJ* 425, L1

Ginzburg V.L., Ozernoy L.M., 1965, *AZh* 42, 943

Girardi L., Bressan A., Chiosi C., Bertelli G., Nasi E., 1996, *A&AS*, 117, 113

Girardi L., Bressan A., Bertelli G., Chiosi C., 2000, *A&AS* 141, 371

Graham J.R., Matthews K., Soifer B.T., Nelson J.E., Harrison W., Jernigan J.G., Lin S., Neugebauer G., Smith G., Ziolkowski C., 1994, *ApJ* 420, L5

Gunn J.E., Peterson B.A., 1965, *ApJ* 142, 1633

Kirkman D., Tytler D., Suzuki N., O'Meara J. M., Lubin D., 2003, *ApJS* 149, 1

Kurucz, R. 1993, ATLAS9 Stellar Atmosphere Programs and 2 km/s grid (Kurucz CD-ROM No.13)

Maeder A., 1992, *A&A* 264, 105

Meynet G., Maeder A., Schaller G., Schaerer D., Charbonnel C., 1994, *A&AS* 103, 97

Miralda-Escudé J., Ostriker J.P., 1990, *ApJ* 350, 1

Mowlavi N., Schaerer D., Meynet G., Bernasconi P. A., Charbonnel C., Maeder A., 1998, *A&A*, 128, 471

Nath B.B., Biermann P.L., 1993, *MNRAS* 265, 241

Ostriker J.P., Ikeuchi S., 1983, *ApJ* 268, L63

Partridge R.B., Peebles P.J.E., 1967, *ApJ* 147, 868

Schaerer D., Charbonnel C., Meynet G., Maeder A., Schaller G., 1993b, *A&A* 102, 339

Schaerer D., Meynet G., Maeder A., Schaller G., 1993a, *A&A* 98, 523

Schaller G., Schaerer D., Meynet G., Maeder A., 1992, *A&AS* 96, 269

Schmidt, M. 1959, *ApJ*, 129, 243

Schwarz J., Ostriker J.P., Yahil A., 1975, *ApJ* 202, 1

Sciama D.W., 1990, *MNRAS* 246, 191

Smith M.S., Kawano L.A., Malaney R.A., 1993, *ApJS* 85, 219

Soifer B.T., Matthews K., Djorgovski S., Larkin J., Graham J.R., Harrison W., Jernigan J.G., Lin S., Nelson J., Neugebauer G., Smith G., Smith J.D., Ziolkowski C., 1994, *ApJ* 420, L1

Songaila A., Cowie L.L., Lilly S.J., 1990, *ApJ* 348, 371

Steidel C.C., 1990, *ApJS* 74, 37

Tegmark M., Silk J., Evrard A., 1993, *ApJ* 417, 54

Traat P., 1996, *AAS* CD-ROM vol. 7.

Tytler D., Kirkman D., O'Meara J. M., Suzuki N., Orin A., Lubin D., Paschos P., Jena T., Lin W.-C., Norman M. L., Meiksin A., 2004, 617, 1

Wagoner R.V., Fowler W.A., Hoyle F., 1967, *ApJ* 148, 3

Walker T.P., Steigman G., Schramm D.N., Olive K.A., Kang H., 1991, *ApJ* 376, 51